Local properties at Fe and Co impurities in $Nb_{1-x}Mo_x$ alloys

R. N. Nogueira and H. M. Petrilli
Instituto de Física, Universidade de São Paulo, Caixa Postal 66318, 05389-970, São Paulo, São Paulo, Brazil
(Received 3 January 1996)

We have investigated the influence of the local environment on the magnetic behavior of substitutional Fe or Co impurities in $Nb_{1-x}Mo_x$ alloys. We have found that the behavior of Fe and Co impurities is very similar in the systems considered here. We have studied the physical mechanisms of the local moment formation at the Fe site in those alloys and discussed what has been suggested in the literature by a different theoretical approach. The isomer shift and hyperfine field at the impurity site have been calculated and compared with experimental data available in the literature. The self-consistent calculations were performed using the real-space linear muffin-tin orbital scheme. [S0163-1829(96)03221-3]

I. INTRODUCTION

The problem of transition-metal impurities in transition-metal hosts is an old and controversial problem that has received renewed attention in the last decade. This renewed interest is due to the fast development of experimental technics and computer facilities, which made rather precise electronic structure calculations feasible. The formation of local magnetic moments at the impurity site in several metallic hosts has been investigated using hyperfine interactions technics such as Mössbauer spectroscopy[1] and time differential perturbed distribution.[2] From the theoretical side supercell calculations,[3] clusters methods,[4] Green's-function technics,[5,6] as well as real-space (RS) methods,[7] have been used to overcome the difficulties introduced by the breakdown of the periodicity in those systems. Such approaches, which use the density-functional theory within the local-spin-density approximation[8] (LSDA) have been often successfully used to study local magnetic and hyperfine properties.

The bcc $Nb_{1-x}Mo_x$ alloys with substitutional Fe or Co impurities forms a very interesting class of alloys where the magnetism at the impurity site depends on the concentration x. It is known from experiment that the impurities are magnetic when $x \geqslant 0.4$ and exhibit no local moment for $x < 0.4$. It is also well known[9] that Fe or Co impurities present local magnetic moment in Mo ($x=1$) but not in Nb ($x=0$). The mechanisms involved in the local moment formation attracts further attention because Nb and Mo are neighbors at the periodic table and both crystallize in the bcc structure. Jaccarino and Walker[10] (JW) have proposed an empirical model where the local magnetism at the impurity site depends on the number of Nb (or Mo) atoms in the first shell of neighbors. The model states that the impurity site would be magnetic if it has not more than one Nb atom as first nearest neighbor (NN). Some calculations for these systems using different theoretical approaches can be found in the literature. At the extreme limits, $x=0$ and $x=1$, that corresponds to the impurities in pure Nb or Mo hosts: (a) one Co impurity has been studied only by the Korringa-Kohn-Rostoker-Green's-function (KKR-GF) method;[11] (b) the behavior of one Fe impurity has been studied by the KKR-GF,[11] the linear-muffin-tin-orbital-atomic-sphere approximation (LMTO-ASA) supercell,[12] and the RS-LMTO-ASA (Ref. 13) approaches. Beuerle, Hummler, and Fähnle[3] is the only group that has investigated theoretically the JW hypothesis. They have used the LMTO-ASA method with a 27 atom supercell to study the case of one Fe impurity in $Nb_{1-x}Mo_x$ alloys. The problem of Co impurities in $Nb_{1-x}Mo_x$ alloys has not yet been considered theoretically in the literature.

The purpose of the present work is to amplify and deepen the understanding of those systems, basically in two different directions. First we study Co as a substitutional impurity in bcc Nb and Mo hosts, comparing its behavior with Fe, its neighbor at the periodic table. From another side we study the local properties at Fe or Co impurities in Nb or Mo hosts, changing their first neighborhood, to simulate some of the possible local environments around the impurity in $Nb_{1-x}Mo_x$ alloys in order to investigate the JW hypothesis. We have chosen three different limiting cases for each host and impurity: only one impurity (Fe or Co) in Mo or Nb hosts; the impurity and one *NN* Mo when the host is Nb or the impurity and one NN Nb when the host is Mo (two impurities problem), and finally the impurity and the whole first Nb shell changed by Mo atoms when the host is Nb, or the first Mo shell changed by Nb atoms when the host is Mo. In all those cases we use the real-space linear muffin-tin orbital in the atomic-sphere approximation (RS-LMTO-ASA) scheme,[14,15] a first-principles approach in the LSDA,[8] especially well suited to investigate local properties, as shown in the literature.[7,13–17] Here we calculate the electronic structure, local magnetic moments, Fermi contact contribution to the hyperfine fields (HF) at the impurities sites, and isomer shifts (IS) when the impurity is Fe. We compare our results with available experimental data and theoretical results obtained by other approaches. We also investigate the local density of states (LDOS) at the Nb or Mo impurity neighbors in each case, in attempt to understand the mechanisms involved in the magnetic moment formation.

The paper is organized as follows: in Sec. II we briefly describe the theoretical method. In Sec. III we present our results and discussions. Finally in Sec. IV we present our conclusions.

II. THEORETICAL APPROACH

In this section we give a brief description of the RS-LMTO-ASA formalism and its application to local perturba-

tions. The RS-LMTO-ASA has been used several times to treat one impurity (substitutional or interstitial) in various hosts. There is also one calculation for more than one impurity in a fcc host.[16] Here the same procedure is applied to the calculation of the electronic structure around more than one substitutional impurity in a bcc host. We also very briefly describe in this section the theoretical approach we use for the calculation of the HF and the IS. A more detailed description of the general procedure can be found elsewhere.[14–16]

The RS-LMTO-ASA is a self-consistent first-principles scheme (without any adjustable parameter) within the density-functional formalism in the framework of the LSDA.[8] It is based on the LMTO-ASA (Ref. 18) formalism but the eigenvalue problem is solved directly in real space using the Cambridge recursion method.[19] The LMTO-ASA method is a linear method and its solutions are more accurate near a freely chosen energy E_ν, usually taken at the center of gravity of the occupied part of the given s, p or d band. Here we use the atomic-sphere approximation (ASA) where the space is divided into Wigner-Seitz (WS) cells, which are then approximated by WS spheres of the same volume centered at each atom. In the RS-LMTO-ASA scheme we use a first-order Hamiltonian, where terms of order $(E-E_\nu)^2$ and higher are neglected. To this approximation we have an orthogonal representation with the Hamiltonian H expressed in terms of tight-binding (TB) parameters. This yields a simple eigenvalue problem, easily solvable in real space by the recursion method,[19] that has the form

$$(H-E)u=0, \tag{1}$$

$$\psi_E(r)=\sum_{R,L}\left[\varphi_{\nu l}(r_R)+(E-E_{\nu lR})\dot{\varphi}_{\nu l}(r_R)Y_L(\hat{r}_R)\right]u_{R,L}(E). \tag{2}$$

Here, the wave function, $\psi_E(r)$, is given in terms of the radial part of the solution of the Schrödinger equation for a spherical potential inside the Wigner-Seitz sphere around each site R, $\varphi_{\nu l}(r_R)$, and its first energy derivative, $\dot{\varphi}_{\nu l}(r_R)$, at E_ν. The values of $\varphi_{\nu l}(r_R)$ and $\dot{\varphi}_{\nu l}(r_R)$ are taken to be zero outside their own sphere. The $Y_L(\hat{r}_R)$ are spherical harmonics, and $u_{R,L}(E)$ are the expansion coefficients of the wave function (2) given by the self-consistent solutions of the eigenvalue problem (1). We note that all inequivalent sites (with different potential parameters) must be considered. The LMTO-ASA can in fact be described as a composition of two self-consistent process, namely the ''general'' and ''atomic'' parts, one inside the other. In the ''general'' process, given the potential parameters for all the inequivalent sites, the Hamiltonian of the system under study is built up and the eigenvalue problem is solved. In the atomic part, the potential parameters, for each inequivalent site, are calculated. The main difference between the present real-space scheme and the usual reciprocal space LMTO-ASA concerns the way by which the eigenvalue problem is solved for the given Hamiltonian. Therefore, the approximations used for the exchange and correlation terms when solving the Schrödinger equation inside the WS spheres are exactly the same in the two approaches. In a periodic system, the Fermi energy (E_F) is determined at each iteration by filling the bands with the correct number of valence electrons. In the case of impurities, the E_F of the system is fixed by the E_F of the host. We calculate the occupation and other moments of the density of states for all nonequivalent sites up to the fixed E_F, keeping the potential parameters of the rest of the system (outside the perturbed region) at bulk value.

After the self-consistent electronic structure for a given system is obtained, the procedure used here for the calculation of HF and IS are the same used in previous papers.[7,13,17,20] Both site-dependent quantities depends on the electronic charge density per spin at the nuclear position, $\rho_\sigma(0)$ where σ denotes spin-up ($\uparrow$) or spin-down ($\downarrow$). To calculate $\rho_\sigma(0)$ we assume that in the vicinity of the nucleus we can expand the charge density in a polynomial series

$$\rho_\sigma(r)=A+Br+Cr^2. \tag{3}$$

From the $\rho_\sigma(0)$ values for the first three radial mesh points we can find the constants A, B, and C, and then $\rho_\sigma(0)$. The total charge density at the nucleus $\rho(0)$ is given by the sum of both $\rho_\sigma(0)$. We note that in the present nonrelativistic calculations only the s orbitals contribute to $\rho(0)$ and we have explicitly calculated the $1s$, $2s$, and $3s$ core contributions as well as the $4s$ valence contribution at the considered site. As shown in the literature, the hyperfine field for transition metals is usually dominated by the Fermi contact contribution that is determined by the magnetization density at the nuclear position R through the expression:

$$\mathrm{HF}_R=\frac{8\pi}{3}\,\mu_B[\rho_R^{\uparrow}(0)-\rho_R^{\downarrow}(0)]. \tag{4}$$

The IS (that can be measured through Mössbauer spectroscopy) can be written as

$$\mathrm{IS}_{\mathrm{imp}}=\alpha[\rho_{\mathrm{imp}}(0)-\rho_{\mathrm{Fe}}(0)] \tag{5}$$

where $\rho_{\mathrm{imp}}(0)$ is the total charge density at the nucleus for the Fe impurity in the systems studied here and $\rho_{\mathrm{Fe}}(0)$ is the same quantity (calculated by the same theoretical method) for a Fe nucleus in pure bcc Fe. Here α is a constant which depends on nuclear properties. This constant is not known, but can be determined by comparisons between the measured and calculated values of the isomer shift for Fe in a series of compounds. Here we use for α the standard value of -0.24 a_0^3 mm s^{-1}.[21] Unfortunately the IS calculations for sites other than Fe (that is, Co, Nb, and Mo) cannot be presently made because of the lack of α values in the literature; there is, to our knowledge, no measured Mössbauer IS values for these atoms. Finally we note that to simplify the notation we will omit throughout this paper the subscripts denoting site for the IS and HF.

III. RESULTS AND DISCUSSION

We present here our results for Fe and Co substitutional impurities in $Nb_{1-x}Mo_x$ alloys. To better understand the magnetic behavior in these systems we have chosen a local approach, looking at three different spatial configurations of atoms in a bcc lattice (among the infinite number of possibilities). For these configurations we establish the following notation:

$\mathbf{A}B = B$ impurity in A host,

$\mathbf{A}(B,C) = B$ and C impurity in A host,

$\mathbf{A}BC_8 = B$ impurity with the first NN shell of C atoms in A host.

In all the cases, the impurity was placed at the position (0,0,0), and in $\mathbf{A}(B,C)$ the second impurity was placed as a NN of the first one at the position (1/2,1/2,1/2). In all nonrelativistic calculations we have used a bcc cluster of 1006 atoms cut in order to keep the atoms of interest at a maximum distance from the surface and lattice parameters that corresponds to Wigner-Seitz radius of 2.992 and 3.053 atomic units for Mo and Nb, respectively. We did not include structural relaxation effects, as their effect are expected to be small in those cases. We have used the Beer-Pettifor[22] terminator and a cutoff parameter $LL=20$ was taken in the recursion chain. The exchange and correlation term of the form proposed by von Barth and Hedin[23] and a basis with nine (s, p, and d) orbitals was used.

To perform a RS-LMTO-ASA calculation for a given system in an efficient way, we need to know which sites are equivalent. As we have mentioned before, we name the sites equivalent if they have the same set of potential parameters. All atoms belonging to the same shell of the impurity neighbors will be equivalent in a bcc lattice with only one impurity. For the systems with two impurities in a bcc lattice, we name two sites i and j equivalent if $d1(i) \equiv d1(j)$ and $d2(i) \equiv d2(j)$, where $d1(i)$ and $d2(i)$ are the distances of the atom i to the impurities 1 and 2, respectively.

We note that the computational efficiency of the calculations can sometimes be improved if the atoms belonging to the perturbed region are not included at once but in a sequential stage: first we calculate the potential parameters for the impurity(ies) site(s) keeping the host atoms potential parameters at the bulk value, stage that we name single site (double site for two impurities); when the impurity reaches self-consistency we start the calculation for the impurity(ies) and its first neighbors keeping the rest of the atoms at the bulk values; in this way we include all different shells of neighbors successively until the whole perturbed region is included. The two impurities procedure is the same as that for systems with only one impurity but we name nth shell the set of atoms belonging to the nth neighborhood of any impurity. We have verified that a perturbed region that includes only the first shell of neighbors gives very reasonable results for the general behavior (LDOS, local moments, HF, IS) at the impurity site in the systems we study here.

A. Local magnetic moments

Here we will focus mainly on two different aspects of the complex problem of local magnetic moment formation at Co or Fe impurities in Mo or Nb hosts. The first one is whether the impurity moment appears or not (whenever this effect can be seen by the LSDA). The second is its dependence on the local atomic configuration for some different environments, simulating the study of its formation at the impurity site in $Nb_{1-x}Mo_x$ alloys.

In Table I we show the presently obtained RS-LMTO-ASA results for the local magnetic moment at the Co site in **Mo**Co and **Nb**Co. We also show the experimental values[9] and the theoretical results obtained with the KKR-GF method[11] available in the literature. From this table we see an excellent agreement of the RS-LMTO-ASA results with both theoretical and experimental results in those cases. We note that the KKR-GF local moment is very sensitive to the angular momentum cutoff l_{max} of the wave functions. Calculations for $l_{max}=2$ yielded large moments for the impurity in both Nb and Mo hosts, and the inclusion of higher angular momenta up to $l_{max}=3$ was necessary to obtain the correct magnetic behavior. As we have observed at the Fe site in **Mo**Fe and **Nb**Fe,[13] our local impurity moments, calculated using a minimum basis of s, p, and d orbitals, are compatible with those obtained via the KKR-GF formalism when a cutoff $l_{max}=3$ is used. At the Fe site in **Mo**Fe, Beuerle *et al.*[12] obtained a local moment of around $2\mu_B$ using an eight atom supercell LMTO-ASA calculation, the KKR-GF (Ref. 11) result is $2.5\mu_B$ and the experimental result is compatible with moments around $2.5\mu_B$. The RS-LMTO-ASA result in this case is $2.5\mu_B$. The slightly smaller local moment obtained by Beuerle *et al.* may be due to the relatively small size of the supercell used to perform the calculations. All three theoretical results show that Fe in **Nb**Fe is nonmagnetic in agreement with the experiment. As it has been pointed out before,[11,12] in a Stoner-like criterion, for a local magnetic moment to appear the condition $I \cdot N(E_F) > 1$ has to be fulfilled.

TABLE I. Calculated local magnetic moments (μ_B) of a single Co impurity in Mo and Nb obtained in this work (RS-LMTO-ASA) compared with theoretical (KKR-GF) and experimental results from Refs. 9 and 11.

	RS-LMTO-ASA	KKR-GF	Expt.
NbCo	0.04	0.0	0.0
MoCo	1.53	1.5	1.6

Here $N(E_F)$ is the paramagnetic local density of states at the Fermi level at the impurity site and I is the Stoner's exchange parameter, that has the LSDA values[24] of 0.072 and 0.068 Ry for Co and Fe, respectively. In order to investigate the fulfilling of this criterion, we have done paramagnetic self-consistent calculations for some of the systems studied here. In Fig. 1 we show our results for the product $I \cdot N(E_F)$ for **Mo**Fe, **Nb**Fe, **Nb**FeMo_8, **Mo**Co, **Mo**(Co,Nb), **Nb**Co, and **Nb**CoMo_8. Following strictly this criterion (as can be seen from Fig. 1) the impurities are expected to be magnetic in **Mo**Fe, **Mo**Co, and **Mo**(Co,Nb). As we shall see,

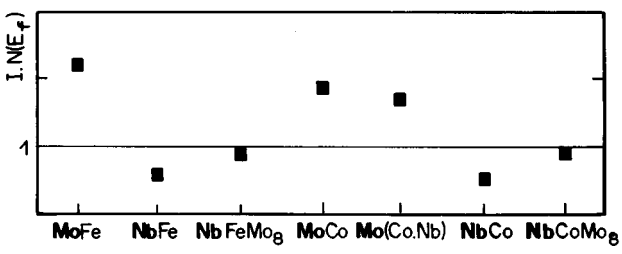

FIG. 1. Paramagnetic local density of states at E_F times I parameter (from Ref. 24) at the impurity site.

TABLE II. Calculated RS-LMTO-ASA local magnetic moments (μ_B) at the Fe or Co sites in the Nb-Mo systems considered here.

	Total	Partial contributions		
		s	*p*	*d*
MoCo	1.53	0.01	0.02	1.50
Mo(Co,Nb)	1.53	0.01	0.01	1.51
Nb$CoMo_8$	0.90	0.00	0.01	0.89
MoFe	2.51	0.02	0.02	2.47
Mo(Fe,Nb)	2.65	0.02	0.02	2.61
Nb$FeMo_8$	2.01	0.01	0.02	1.98

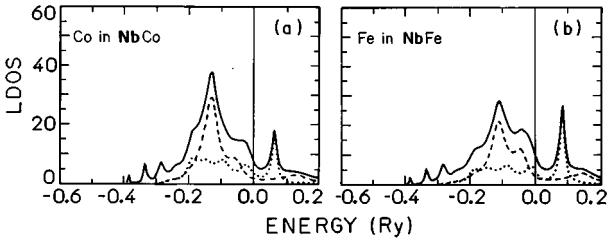

FIG. 2. Calculated RS-LMTO-ASA local density of states (states/Ry atom spin) in (a) Co and (b) Fe impurity sites in the Nb host. Solid line: full local density of states; dashed line: contribution of T_{2g} states; dotted line: contribution of E_g states. The vertical line denotes the Fermi level.

Fe and Co behave in a very similar way in all the systems presently studied so, although we have not done a paramagnetic calculation for **Mo**(Fe,Nb), we expect the Fe impurity also to be magnetic in **Mo**(Fe,Nb). The impurities in **Nb**$FeMo_8$ and **Nb**$CoMo_8$ almost fulfill the Stoner-like criterion. We note that the recursion method that is usually very reliable for the calculation of integrated quantities such as occupations, magnetic moments, charge transfers, etc., gives only the qualitative features and general shape of the LDOS. Therefore we do not expect to obtain a very precise value for $N(E_F)$, the LDOS at the Fermi level.

As a third step in our analysis, we have done self-consistent spin-polarized RS-LMTO-ASA calculations for the 12 systems. Our results shows that there is no local magnetic moment formation at the impurity site for **Nb**Co, **Nb**(Fe,Mo), **Nb**(Co,Mo), **Mo**$FeNb_8$, **Mo**$CoNb_8$; also no local moment at **Nb**Fe has been observed (Ref. 13). In Table II we show the values that we have obtained for the local magnetic moments at Co or Fe impurities in **Mo**Co, **Mo**(Co,Nb), **Nb**$CoMo_8$, **Mo**Fe, **Mo**(Fe,Nb), and **Nb**$FeMo_8$. We also show the *s*, *p*, and *d* partial contributions to the local magnetic moment. Comparing Fig. 1 and Table II we can see that whenever the Stoner-like criterion has strictly been fulfilled, we have observed a local magnetic moment at the impurity site. The only exceptions are **Nb**$FeMo_8$ and **Nb**$CoMo_8$ where Table II shows a significant value for the local moments obtained from the self-consistent spin-polarized calculations but Fig. 1 shows that the Stoner-like criterion is in the border region of being fulfilled. Although we do not expect the RS-LMTO-ASA to describe precisely the details of the LDOS at the Fermi level, as we shall see below, those systems are in a region of very unstable magnetic behavior.

The JW empirical model states that, whenever the impurity (Fe or Co) in $Nb_{1-x}Mo_x$ alloys does not have more than one Nb NN, the impurity presents a fixed value for the local moment; otherwise it does not show a local moment, independent of the kind of further distant atoms. Looking at Table II we see that the substitution of a NN does not change the impurity moment, in agreement with this empirical model. The results for systems without local impurity moment (**Mo**$CoNb_8$ and **Mo**$FeNb_8$) are also in agreement with the JW hypothesis. Now, the results for the impurity moment in **Nb**$CoMo_8$ and **Nb**$FeMo_8$ are slightly different from those found for the isolated impurity, showing that the impurity moment depend to some degree on the kind of further distant atoms. Beuerle, Hummler, and Faähnle[3] observed a very rapid Fe moment collapse with increasing number of NN Nb atoms, in general agreement with our results. But in contrast, they have found a small decrease of the Fe local moment at the inclusion of one Nb NN in the Mo host [**Mo**(Fe,Nb)] and they mention a collapse of the Fe moment in $NbFeMo_8$. In those calculations they have used the LMTO-ASA method but with a 27 atom supercell to simulate the alloys. The main difference between the approach used by Beuerle *et al.* and the one we use here is on the way by which the whole solid is described: the supercell has a defect that is repeated throughout the solid and the real space has only one perturbed region in a given host. In highly sensitive magnetic situations the interaction between the defects charges can lead to different results obtained by the two approaches. In order to further check this situation it would be interesting if LMTO-ASA supercell calculations would be performed for the $Nb_{1-x}Mo_x$ alloys with Co impurity.

To get further into the discussion of the mechanisms involved in the local moment formation in the compounds under study, we make an analysis of the LDOS at impurity and NN sites. Beuerle *et al.*[12] have investigated the LDOS for Fe impurities in pure bcc transition-metal hosts, and suggested that the interaction between host and impurity states with T_{2g} (xy,xz,yz) symmetry, is mainly responsible for the formation of the impurity local moment. Here we basically follow their approach trying to verify if their conclusions for the Fe impurity can be extended to the Co case. To make the discussion more transparent we present plots of the total LDOS at each site and also the projected LDOS with $E_g(3z^2-r^2,x^2-y^2)$ and T_{2g} symmetry; in all the following pictures we take E_F as the zero of energy. In both presently obtained LDOS for pure bcc Nb and Mo we see essentially a four-peak structure: the lower energy peak of mixed (T_{2g} and E_g) character, two intermediate peaks dominated by T_{2g} states and the highest energy peak (mostly unoccupied) dominated by E_g states. The general shape of the Mo and Nb LDOS is the same, but as Mo has one more electron, its E_F is higher, and is located in a LDOS valley between the highest peak (dominated by E_g symmetry) and the peaks dominated by T_{2g} states; the Nb E_F is in the region dominated by the peaks of the T_{2g} states. Those features are in very good agreement with Ref. 12 but the exact details of the LDOS are not so well described by the recursion method.

We now compare the systems with one Co or Fe impurity in the Nb or Mo host. In Fig. 2 we show the paramagnetic LDOS at the Co and Fe site in the Nb host. We see that their shape are very similar, mainly with a two peak structure: the first one, below E_F, dominated by T_{2g} states and the other

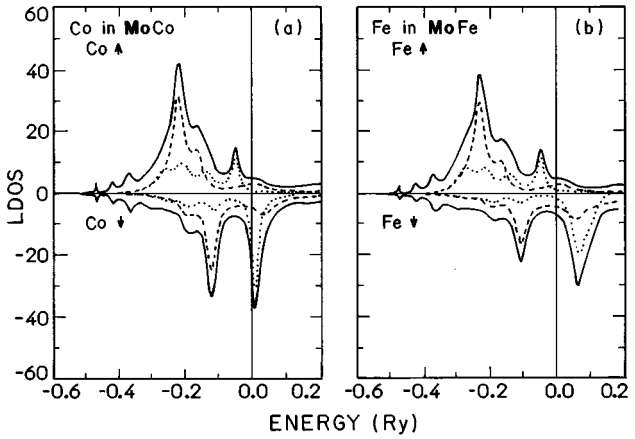

FIG. 3. Calculated RS-LMTO-ASA spin-polarized local density of states (states/Ry atom spin) at (a) Co and (b) Fe impurity sites in the Mo host. Solid line: full local density of states; dashed line: contribution of T_{2g} states; dotted line: contribution of E_g states. The vertical line denotes the Fermi level.

located above E_F dominated by E_g symmetry states. The Co peaks are slightly higher than in Fe and E_F is slightly shifted to higher energies in order to include one more electron in the occupied band region. If we now compare the paramagnetic LDOS at the Fe and Co impurities in Mo with the ones in the Nb host (Fig. 2) we observe that there is a redistribution of the states: the peak dominated by T_{2g} symmetry states becomes narrower and the one dominated by E_g symmetry becomes higher and shifts to a region around E_F. The location of one Co or Fe peak at E_F according to Stoner-like models, leads to a local magnetic moment. In Figs. 3(a) and 3(b) we show the self-consistent spin-polarized LDOS for the Co or Fe impurities in Mo. The splitting of the bands occurs with significant changes of their shapes (compared to the paramagnetic ones), specially for the Fe case. We can also note that the most occupied bands shows a larger shape variation; as they are shifted to lower energies, they interact more with the host states in a energy region where Mo has a larger number of states. The minority-spin LDOS resembles the paramagnetic LDOS in both cases, but in Fe we see a broadening of the peaks relative to those in Co. As the majority band is almost full in both cases, in order to maintain the correct number of states, the Fe impurity requires a larger splitting of the bands and Fe has a local magnetic moment

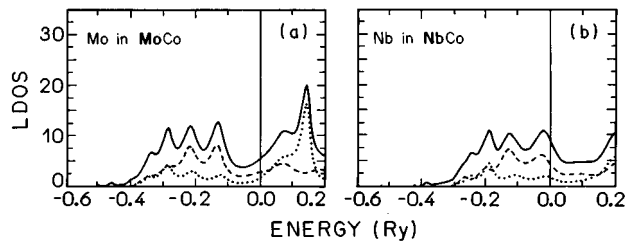

FIG. 4. Calculated RS-LMTO-ASA local density of states (states/Ry atom spin) for (a) Mo and (b) Nb nearest-neighbor of the Co impurity in the Mo and Nb host, respectively. Solid line: full local density of states; dashed line: contribution of T_{2g} states; dotted line: contribution of E_g states. The vertical line denotes the Fermi level.

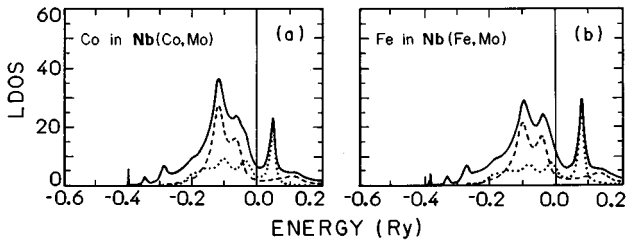

FIG. 5. Calculated RS-LMTO-ASA local density of states (states/Ry atom spin) at (a) Co and (b) Fe impurity sites in the Nb host with one nearest neighbor Mo. Solid line: full local density of states; dashed line: contribution of T_{2g} states; dotted line: contribution of E_g states. The vertical line denotes the Fermi level.

$1\mu_B$ larger than Co. This larger splitting causes a redistribution of the Fe minority-spin states, since they are interacting with the states of the Mo host in a different energy region (note that E_F is located in a valley of the Mo host LDOS).

It is interesting to note the strong effect of the Mo host on the impurity LDOS. Just for completeness, following the trend of Fe and Co impurities, we have made calculations for the Ni impurity in the Mo host (**Mo**Ni). The shape of the Fe, Co, and Ni LDOS in the Mo host is almost the same, just moving to lower energies in order to add one more electron. At the Ni case, E_F is above the E_g peak, in a region of low LDOS, and in agreement with Stoner-like models, Ni presents no local magnetic moment in **Mo**Ni. We can also say that the trend observed for the minority-spin LDOS is that it becomes even more similar to the paramagnetic LDOS as we go from Fe to Co and Ni, filling the band.

If we now compare the LDOS at the Co first NN Nb or Mo site in **Nb**Co and **Mo**Co shown in Fig. 4 with the correspondent pure hosts we observe that the presence of the Co impurity affects very little the host LDOS. We note that, in all systems presently studied the effect of Fe and Co impurities over the LDOS of its first neighbors is very similar. Therefore here we will present only plots of the results for Co first-neighbor shell.

We now consider the systems Fe or Co impurities in the Mo and Nb host but with one NN changed, that is **Nb**-

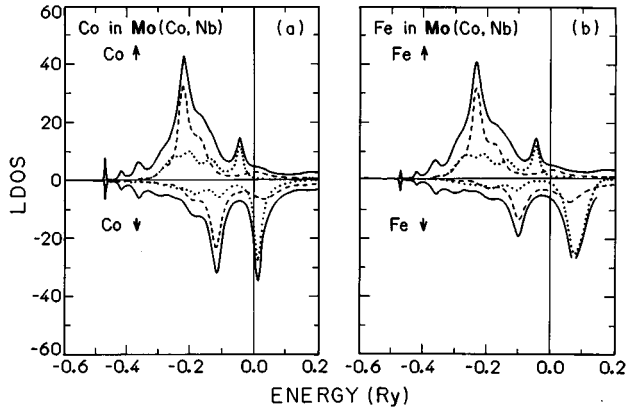

FIG. 6. Calculated RS-LMTO-ASA spin-polarized local density of states (states/Ry atom spin) at (a) Co and (b) Fe impurity sites in the Mo host with one nearest neighbor Nb. Solid line: full local density of states; dashed line: contribution of T_{2g} states; dotted line: contribution of E_g states. The vertical line denotes the Fermi level.

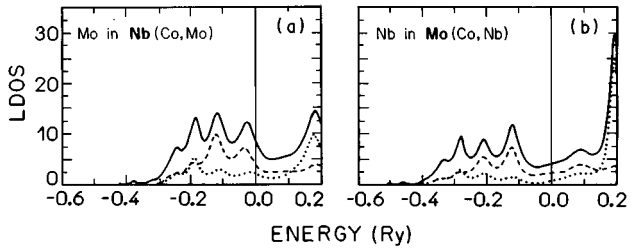

FIG. 7. Calculated RS-LMTO-ASA local density of states (states/Ry atom spin) for the two impurities systems for (a) Mo and (b) Nb nearest neighbors of the Co impurity in the Nb and Mo host, respectively. Solid line: full local density of states; dashed line: contribution of T_{2g} states; dotted line: contribution of E_g states. The vertical line denotes the Fermi level.

(Co,Mo), **Nb**(Fe,Mo), **Mo**(Co,Nb), and **Mo**(Fe,Nb). In Fig. 5 we show the Co and Fe LDOS in **Nb**(Co,Mo) and **Nb**(Fe,Mo). We can see that the LDOS for the impurities with one first NN Mo in the Nb host resembles very much the ones of the isolated impurities in Nb (fig. 2). In the same way, the spin-polarized LDOS for the impurities in Mo host with one first NN Nb shown in Fig. 6 also remains very similar to the isolated impurities in Mo [Figs. 3(a) and 3(b)]. To understand this behavior we show in Fig. 7 the LDOS at the Mo and Nb atoms that have been exchanged by the Nb and Mo host atoms in **Nb**(Co,Mo) and **Mo**(Co,Nb), respectively. We see that both Mo and Nb impurities have their LDOS shifted in order to become concentrated in the same energy region of the host atom that was previously in the considered site (Fig. 4). The difference between the impurity occupation and that of the host (due to the fact that Mo has one more electron) leads only to a different height of the LDOS peaks. Since the LDOS of this atom becomes similar to the original host, the impurity will not be very affected by this NN substitution. This explains why the impurity local magnetic moment remains the same when only one of its NN is exchanged.

We now substitute all the atoms from the impurity first NN shell in the Mo host by Nb atoms and in the Nb host by Mo atoms (the systems **Mo**$CoNb_8$, **Mo**$FeNb_8$, **Nb**$CoMo_8$, and **Nb**$FeMo_8$. The Co and Fe impurity LDOS in those systems are shown in Figs. 8 and 9. The paramagnetic Co and Fe LDOS keep only some resemblance with the general shape of the LDOS for one isolated impurity in the same

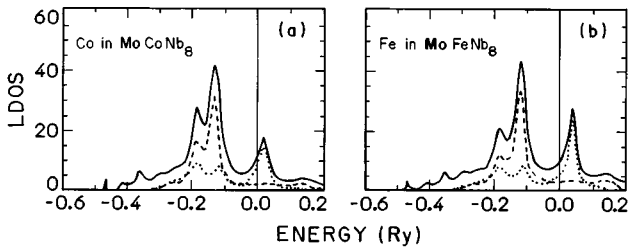

FIG. 8. Calculated RS-LMTO-ASA local density of states (states/Ry atom spin) at (a) Co and (b) Fe impurity sites in the Mo host with all atoms of the first-nearest-neighbor shell Nb. Solid line: full local density of states; dashed line: contribution of T_{2g} states; dotted line: contribution of E_g states. The vertical line denotes the Fermi level.

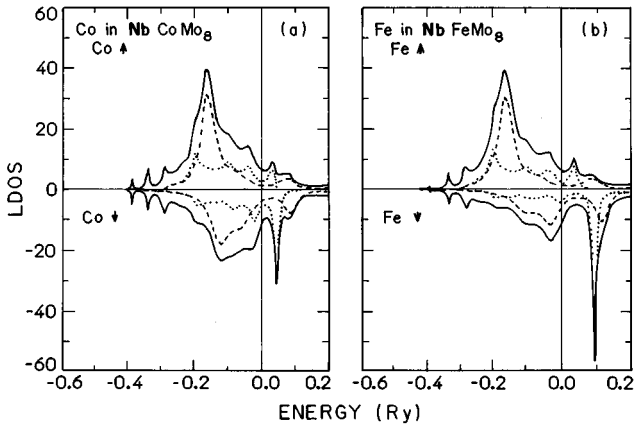

FIG. 9. Calculated RS-LMTO-ASA spin-polarized local density of states at (a) Co and (b) Fe impurity sites in the Nb host with all atoms of the first-nearest-neighbor shell Mo. Solid line: full local density of states; dashed line: contribution of T_{2g} states; dotted line: contribution of E_g states. The vertical line denotes the Fermi level.

host. We can roughly say that they have a mixed character, between the cases where Mo and Nb are hosts. Specifically in the cases **Nb**$FeMo_8$ and **Nb**$CoMo_8$, we observe a strong magnetic instability situation, which becomes clear in a Stoner-like criterion analysis (see Fig. 1). Both present a magnetic splitting of the bands [Figs. 9(a) and 9(b)] forming a local magnetic moment. The LDOS of the Mo and Nb impurity NN in **Nb**$CoMo_8$ and **Mo**$CoNb_8$ are shown in Fig. 10. We observe that, still in this situation their LDOS tends to resemble the LDOS of those atoms they have substituted (Fig. 4), although not as much in the case where only one NN has been substituted (Fig. 7). This remaining resemblance can be explained by the fact that this atom (Fig. 10) has one Co (or Fe) atom plus seven host atoms in its first neighborhood; in the second neighborhood it has three atoms of its same type and three of the host type, the remaining atoms of its same type belonging to its third (three atoms) and fifth (one atom) neighborhood. In this case, the considered atom in Fig. 10 will still interact essentially with the host atoms.

B. Hyperfine interactions

We now get into the analysis of the usually dominant Fermi contact contribution to the hyperfine field (HF) at the Fe and Co impurities in the systems considered above. In

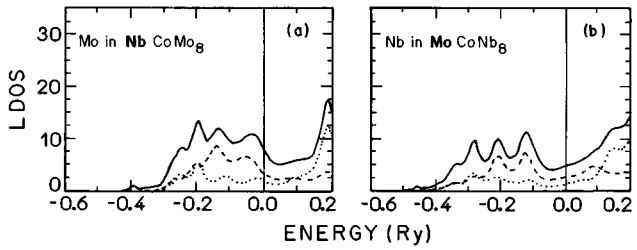

FIG. 10. Calculated RS-LMTO-ASA local density of states for (a) Mo (shell) and (b) Nb (shell) nearest neighbors of the Co impurity in the Nb and Mo host, respectively. Solid line: full local density of states; dashed line: contribution of T_{2g} states; dotted line: contribution of E_g states. The vertical line denotes the Fermi level.

TABLE III. Calculated RS-LMTO-ASA hyperfine fields (T) at the Fe or Co impurity sites in the Nb-Mo systems considered here.

	Core			Total core	Valence	Total
	1*s*	2*s*	3*s*		4*s*	
MoCo	−2.1	−35.8	22.3	−15.6	6.7	−8.9
Mo(Co,Nb)	−2.4	−36.1	22.5	−16.0	6.7	−9.3
Nb$CoMo_8$	−0.9	−21.2	13.2	−9.0	3.8	−5.2
MoFe	−0.4	−52.6	30.8	−22.2	10.9	−11.3
Mo(Fe,Nb)	−2.2	−55.6	32.6	−25.2	12.6	−12.6
Nb$FeMo_8$	−3.4	−42.0	24.5	−20.9	9.8	−11.1

TABLE IV. Calculated RS-LMTO-ASA isomer shifts (mm/s) at the Fe sites in the Nb-Mo systems considered here.

	IS
MoFe	0.08
Mo(Fe,Nb)	0.10
Mo$FeNb_8$	0.00
NbFe	0.05
Nb(Fe,Mo)	0.08
Nb$FeMo_8$	0.10

Table III we show our results for the core, valence and total contributions to the HF's at the impurity (Co or Fe) site in **Mo**Co, **Mo**(Co,Nb), **Nb**$CoMo_8$, **Mo**(Fe,Nb), **Nb**$FeMo_8$, and the **Mo**Fe previously obtained in Ref. 13. The experimental results available in the literature are −11.2 T (Ref. 25) and −2.6 T (Ref. 26) for Fe in **Mo**Fe and Co in **Mo**Co, respectively. Comparing these values with the ones at Table III we observe an excellent agreement between experimental and theoretical values in the **Mo**Fe case but only a qualitative agreement in the **Mo**Co case. In **Mo**Co the obtained value is smaller than in **Mo**Fe following the experimental trend, but the magnitude differs by around 6 T. We note that this small measured value for the HF at the Co site is quite unusual as pointed out by Brog, Jones, and Booth;[27] to get deeply into this question we will investigate if the results are compatible with the possibility of Co cluster formation in Mo-Co alloys in a future paper. We remember however that the HF is a very subtle quantity that depends on very small differences of large numbers, being in fact a test of the accuracy that can be reached by a given theoretical approach. If we compare the HF at Table III with the local magnetic moments shown at Table II we can observe that the core contribution to the HF is always proportional to the local magnetic moment at that site, with a proportionality constant around −10 T. The valence contribution has opposite sign to the core contribution and, although in a less pronounced way, is proportional to the local 4*s* moment at the corresponding site. Those trends are in agreement with what has been observed by Bluegel, *et al.*[28] performing KKR-GF calculations for 3*d* and 4*d* impurities in Ni. Following the same trend observed for the local moment, the values of the HF at the impurity (as well as their partial contributions) in the various systems shown at Table III are not affected by the substitution of only one Mo NN by a Nb atom. On the other hand, when we have all the impurity first NN Mo in Nb host, we see that every contribution is affected, what indicates that the second NN shell may influence the HF value. In **Nb**$FeMo_8$ we see a particular cancelation of these effects that leads to the same HF as in **Mo**Fe; this very special situation is not seen in **Nb**$CoMo_8$.

Finally we consider the IS at the Fe sites shown in Table IV. The **Mo**Fe and **Nb**Fe results are in excellent agreement with the measured values as already discussed in Ref. 13. In all the situations considered here, the IS values presented at Table IV are very similar and with a small magnitude. This fact indicates that Fe sites in $Nb_{1-x}Mo_x$ will show a small IS as a general rule. We note that this very small magnitude is near to the limit of precision that can be reached by our theoretical approach.

IV. CONCLUSIONS

We have used the RS-LMTO-ASA scheme to study the local behavior around Co or Fe impurities in $Nb_{1-x}Mo_x$ alloys. For that purpose we have choosen three possible spatial configurations for the impurity nearest neighborhood. We have found that the Co behavior is in all cases very similar to that of the Fe. Our analysis of the impurity first neighborhood has shown that, important for the magnetic behavior in those systems is the fact that, when exchanged, both Mo and Nb tend to resemble the host atoms they substitute.

Beuerle *et al.*[12] suggests that the $T_{2g}-T_{2g}$ interaction between the impurity and its NN play an important role in the local magnetic moment formation. Our results confirms the importance of this mechanism for the Fe impurity and shows that the same analysis is valid for Co. We observe that the substitution of one impurity NN does not change the impurity local moment and the systems where it has all NN Nb, even in Mo host, remained nonspin polarized; the local moment at impurities with all NN Mo presented some influence from further neighborhoods. We have found a local moment at the Fe site in **Nb**$FeMo_8$ in contrast with LMTO-ASA supercell calculations (Ref. 3). Although we have locally the same environment, those schemes describes in different way the bulk system and the differences between the two approaches should be further investigated.

We found a small IS at all Fe sites indicating an always small value in $Nb_{1-x}Mo_x$ alloys. Our calculated values for the HF has shown that, as in the local moment case, the exchange of one impurity NN does not affect the HF magnitude, but the HF is sensitive to the concentration and may be used to label different environments.

ACKNOWLEDGMENTS

We wish to thank Dr. S. Frota-Pessôa for very useful discussions and careful reading of the manuscript. This work was partially supported by Fundação de Amparo à Pesquisa do Estado de São Paulo (FAPESP), Conselho Nacional de Desenvolvimento Cientiífico e Technológico (CNPq) and Financiadora de Estudos e Projectos (FINEP).

[1] Y. Yoshida *et al.*, Phys. Rev. Lett. **61**, 195 (1988); for a recent review, see R. Sielemann and Y. Yoshida, Hyperfine Interact. **68**, 119 (1991).
[2] D. Riegel *et al.*, Phys. Rev. Lett. **62**, 316 (1989); K. D. Gross, D. Riegel, and R. Zeller, *ibid*. **65**, 3044 (1990); for a recent review, see D. Riegel and K. D. Gross, Physica (Amsterdam) **163B**, 678 (1990).
[3] T. Beuerle, K. Hummler, and M. Fähnle, Int. J. Mod. Phys. B **7**, 756 (1993).
[4] D. Guenzburger and D. E. Ellis, Phys. Rev. Lett. **67**, 3832 (1991).
[5] R. J. Braspenning, R. Zeller, A. Ludder, and P. H. Dederichs, Phys. Rev. B **29**, 703 (1984).
[6] C. Koenig, N. Stefanou, and J. M. Koch, Phys. Rev. B **33**, 5307 (1986).
[7] S. Frota-Pessôa, L. A. de Mello, H. M. Petrilli, and A. B. Klautau, Phys. Rev. Lett. **71**, 4206 (1993).
[8] P. Hohenberg and W. Kohn, Phys. Rev. **136**, B864 (1964); W. Kohn and L. J. Shan, *ibid*. **140**, A1133 (1965); O. Gunnasson and B. I. Lundgvist, Phys. Rev. B **13**, 4274 (1976).
[9] K. C. Brog and W. H. Jones, Jr., Phys. Rev. Lett. **24**, 58 (1970); K. C. Brog, W. H. Jones, Jr., and G. S. Knapp, Solid State Commun. **5**, 913 (1967); B. B. Schwartz and R. B. Frankel, in *Mössbauer Effect Methodology*, edited by I. J. Gruverman (Plenum, New York, 1971), Vol. 7; N. I. Krivko, Sov. Phys. Solid State **11**, 334 (1969).
[10] V. Jaccarino and L. R. Walker, Phys. Rev. Lett. **15**, 258 (1965).
[11] P. Lang, B. Drittler, R. Zeller, and P. H. Dederichs, J. Phys. Condens. Matter **4**, 911 (1992).
[12] T. Beuerle, K. Hummler, C. Elsässer, and M. Fähnle, Phys. Rev. B **49**, 8802 (1994).
[13] H. M. Petrilli and S. Frota-Pessôa, Phys. Rev. B **48**, 7148 (1993).
[14] S. Frota-Pessôa, Phys. Rev. B **46**, 14 570 (1992).
[15] P. R. Peduto, S. Frota-Pessôa, and M.S. Methfessel, Phys. Rev. B **44**, 13 283 (1991).
[16] S. Ferreira and S. Frota-Pessôa, Phys. Rev. B **51**, 2045 (1995).
[17] H. M. Petrilli and S. Frota-Pessôa, Hyperfine Interact. **78**, 377 (1993).
[18] O. K. Andersen, Phys. Rev. B **12**, 3060 (1975); O. K. Andersen and O. Jepsen, Phys. Rev. Lett. **53**, 2571 (1984); O. K. Andersen, O. Jepsen, and D. Glötzel, in *Highlights of Condensed Matter Theory*, edited by F. Bassani, F. Funi, and M. P. Tosi (North-Holland, Amsterdam, 1985).
[19] R. Haydock, in *Solid State Physics: Advances in Research and Applications*, edited by H. Ehrenreich, F. Seitz, and D. Turnbull (Academic, New York, 1980), Vol. 35, p. 216.
[20] H. M. Petrilli and S. Frota-Pessôa, Hyperfine Interact. **83**, 239 (1994).
[21] A. Akai *et al.*, Phys. Rev. Lett. **56**, 2407 (1986).
[22] N. Beer and D. Pettifor, in *Electronic Structure of Complex Systems*, edited by W. Temmerman and P. Phariseau (Plenum, New York, 1984).
[23] V. von Barth and L. Hedin, J. Phys. C **5**, 1629 (1972).
[24] J. P. Janak, Phys. Rev. B **16**, 255 (1977).
[25] D. Riegel, L. Büermann, K. D. Gross, M. Luszik-Bhadra, and S. N. Misha, Phys. Rev. Lett. **62**, 316 (1989).
[26] A. Narath, Phys. Rev. B **13**, 3724 (1976).
[27] K. C. Brog, W. H. Jones, and J. G. Booth, J. Appl. Phys. **38**, 1151 (1967).
[28] S. Blügel, H. Akai, R. Zeller, and P. H. Dederichs, Phys. Rev. B **35**, 3271 (1987).